

## METHODOLOGY

---

Gerald C. Nelson, Amanda Palazzo, Daniel Mason-d’Croz,  
Richard Robertson, and Timothy S. Thomas

**M**odeling the impacts of climate change on agriculture presents a complex challenge arising from the wide-ranging processes underlying the working of markets, ecosystems, and human behavior. The analytical framework used in this monograph integrates modeling components that range from the macro to the micro to model a range of processes, from those driven by economics to those that are essentially biological in nature. This chapter brings together in one place the technical details associated with models used in this monograph along with other technical information that is common to most or all of the chapters. Figure 2.1 provides a diagram of the links among the three models used: the International Food Policy Research Institute’s (IFPRI’s) International Model for Policy Analysis of Agricultural Commodities and Trade (IMPACT) model (Rosegrant et al. 2008) a partial equilibrium agriculture model that emphasizes policy simulations; a hydrology model incorporated into IMPACT; and the Decision Support Software for Agrotechnology Transfer (DSSAT) crop model suite (Jones et al. 2003) that estimates yields of crops in varying management systems and climate change scenarios.

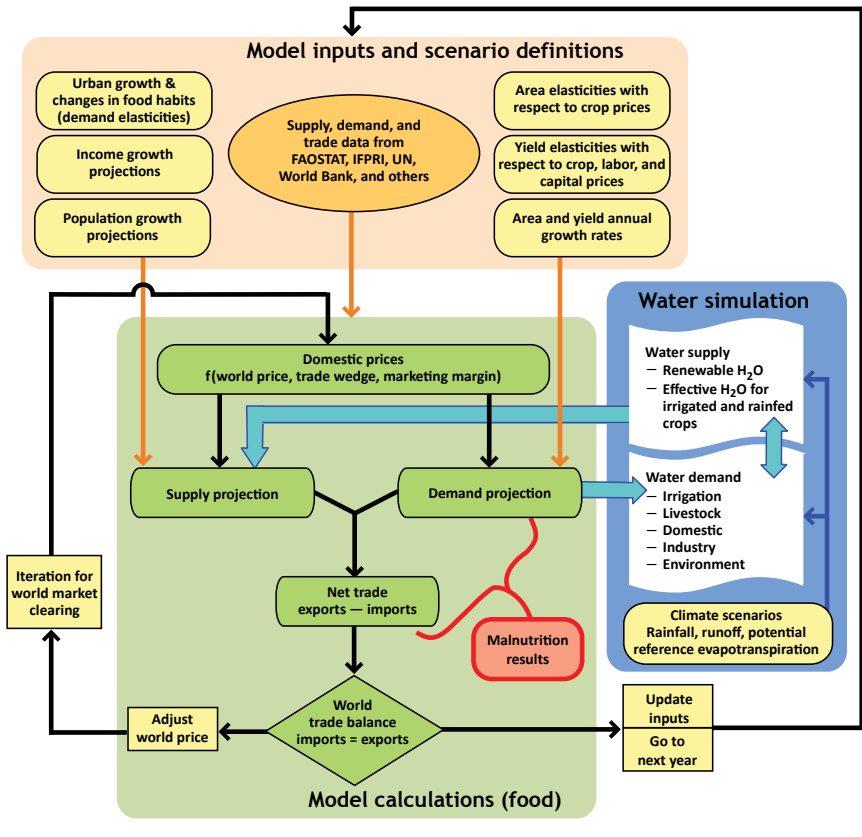
### **General Circulation Models (GCMs) and Climate Scenarios**

GCMs model the physics and chemistry of the atmosphere and its interactions with oceans and the land surface. Several GCMs have been developed independently around the world. For the Fourth Assessment Report (AR4) of the Intergovernmental Panel on Climate Change (IPCC), 23 GCMs made some model results publicly available. Results from four are used in this monograph.

---

This chapter draws heavily on Nelson et al. (2010).

**FIGURE 2.1** The International Model for Policy Analysis of Agricultural Commodities and Trade (IMPACT) modeling framework



Source: Nelson et al. (2010)

Note: FAO/STAT = FAO/STAT Database on Agriculture (FAO 2010); IFPRI = International Food Policy Research Institute; UN = United Nations.

The GCMs create estimates of precipitation and temperature values around the globe often at something close to 2-degree intervals (about 200 kilometers at the equator) for most models. This is very coarse and may hide important differences on a more local scale. In order to have finer resolution, it is common to “downscale” the data. Data downscaled by Jones, Thornton, and Heinke (2009) provide precipitation and temperature data at a 5 arc-minute resolution (around 9 kilometers at the equator, smaller away from it, which is called “10-kilometer resolution” in this monograph).

Greenhouse gas emissions alter atmospheric chemistry, ultimately increasing temperatures and altering precipitation patterns. AR4 had three scenarios

of greenhouse gas emissions pathways: B1, A1B, and A2.<sup>1</sup> Scenario B1 was a low-emissions scenario, which by 2011 does not appear to be very realistic. Scenarios A2 and A1B are higher emission scenarios, with similar trajectories through 2050 but different ones after 2050. Because this monograph is primarily concerned with changes between now and 2050, we elected to focus on scenario A1B when presenting the biophysical effects on crop yields, but we used both B1 and A1B in the IMPACT model in order to give a wider range of scenario outcomes.

To illustrate the range of potential effects on crops, we used results from four GCMs, CNRM-CM3, CSIRO Mark 3, ECHAM 5, and MIROC 3.2 medium resolution.<sup>2</sup> For inputs into the IMPACT model, results from only two GCMs were used, the CSIRO Mark 3 and the MIROC 3.2 medium-resolution models. The rationale for doing that can be seen more clearly in Table 2.1, in which we see that the lowest levels of precipitation change and lowest levels of temperature change are given by the CSIRO GCM and the highest levels of precipitation and temperature change are given by the MIROC GCM.

In the country analyses in the other chapters of this monograph, we display two kinds of maps that show spatially differentiated predictions of the GCMs. One shows changes in annual rainfall, and the other shows changes in the mean daily maximum temperature for the warmest month. The changes in the latter are determined by finding the month in 2000 with the highest mean daily maximum temperature and subtracting that mean value from the mean value for the month with the highest mean daily maximum temperature for 2050.

### **The Spatial Production Allocation Model (SPAM)**

SPAM is a set of raster datasets showing harvest area, production, and yield for 20 crops or aggregates of crops and for three management systems

---

1 B1 is a greenhouse gas emissions scenario that assumes a population that peaks midcentury (like A1B), but with rapid changes toward a service and information economy, and the introduction of clean and resource-efficient technologies. A1B is a greenhouse gas emissions scenario that assumes fast economic growth, a population that peaks midcentury, and the development of new and efficient technologies, along with a balanced use of energy sources. A2 is a greenhouse gas emissions scenario that assumes a very heterogeneous world with continuously increasing global population and regionally oriented economic growth that is more fragmented and slower than in other storylines (Nakicenovic et al. 2000).

2 CNRM-CM3 is National Meteorological Research Center–Climate Model 3. CSIRO Mark 3 is a climate model developed at the Australia Commonwealth Scientific and Industrial Research Organisation. ECHAM 5 is a fifth-generation climate model developed at the Max Planck Institute for Meteorology in Hamburg. MIROC 3.2 is the Model for Interdisciplinary Research on Climate, developed at the University of Tokyo Center for Climate System Research.

**TABLE 2.1** GCM and SRES scenario global average changes, 2000–2050

GCM	SRES scenario	Change between 2000 and 2050 in the annual averages			
		Precipitation (percent)	Precipitation (millimeters)	Minimum temperature (°C)	Maximum temperature (°C)
<b>CSIRO</b>	<b>B1</b>	<b>0.0</b>	<b>0.1</b>	<b>1.2</b>	<b>1.0</b>
<b>CSIRO</b>	<b>A1B</b>	<b>0.7</b>	<b>4.8</b>	<b>1.6</b>	<b>1.4</b>
CSIRO	A2	0.9	6.5	1.9	1.8
ECHAM 5	B1	1.6	11.6	2.1	1.9
CNRM-CM3	B1	1.9	14.0	1.9	1.7
ECHAM 5	A2	2.1	15.0	2.4	2.2
CNRM-CM3	A2	2.7	19.5	2.5	2.2
ECHAM 5	A1B	3.2	23.4	2.7	2.5
MIROC	A2	3.2	23.4	2.8	2.6
CNRM-CM3	A1B	3.3	23.8	2.6	2.3
<b>MIROC</b>	<b>B1</b>	<b>3.6</b>	<b>25.7</b>	<b>2.4</b>	<b>2.3</b>
<b>MIROC</b>	<b>A1B</b>	<b>4.7</b>	<b>33.8</b>	<b>3.0</b>	<b>2.8</b>

Source: Nelson et al. (2010).

Notes: In this table and elsewhere in the text, a reference to a particular year for a climate realization, such as 2000 or 2050, in fact refers to mean values around that year. For example, the data described as 2000 in this table are representative of the period 1950–2000. The data described as 2050 are representative of the period 2041–2060. GCM scenario combinations in bold are the ones used in the climate scenario analysis. A1B = greenhouse gas emissions scenario that assumes fast economic growth, a population that peaks midcentury, and the development of new and efficient technologies, along with a balanced use of energy sources; B1 = greenhouse gas emissions scenario that assumes a population that peaks midcentury (like A1B), but with rapid changes toward a service and information economy, and the introduction of clean and resource-efficient technologies; CNRM-CM3 = climate model developed by the National Meteorological Research Center; CSIRO = climate model developed at the Australia Commonwealth Scientific and Industrial Research Organisation; ECHAM 5 = fifth-generation climate model developed at the Max Planck Institute for Meteorology (Hamburg); GCM = general circulation model; MIROC = Model for Interdisciplinary Research on Climate, developed by the University of Tokyo Center for Climate System Research; SRES = Special Report on Emissions Scenarios, a report by the Intergovernmental Panel on Climate Change that was published in 2000.

(irrigated, high-input rainfed, and low-input rainfed, with the latter two combined in this monograph to make a rainfed total). The model employs a cross-entropy approach to manage inputs with different levels of likelihood in indicating the specific locations of agricultural production (You and Wood 2006; You, Wood, and Wood-Sichra 2006, 2009).

SPAM spatially allocates crop production from large reporting units (administrative units such as province or district level) to a raster grid at a spatial resolution of 5 arc-minutes. The allocation model works by inferring likely production locations from multiple indicators that, in addition to subnational crop production statistics, also include satellite data on land cover, maps of

irrigated areas, biophysical crop suitability assessments, population density, and secondary data on irrigation and rainfed production.

In some of the maps presented in this monograph, SPAM areas are reported in units of hectares per raster cell. A 5-arc-minute grid cell is just over 8,500 hectares at the equator, which is a reasonable value to use when gauging how great a proportion of the cell might be used by the crop shown in the map.

SPAM areas are used to provide weights for calculating provincial and national yield changes due to climate change in the regional overview chapter. Cells with greater current levels of that crop are weighted higher when aggregating the crop model results. This was also the approach used for aggregating crop model results to the national level for use in the IMPACT model.

## **DSSAT**

DSSAT is a software package used for modeling crop production (Jones et al. 2003). The software “grows” the crop in daily time increments, and therefore daily weather data are required. With climate models, we have only monthly statistics on the weather. DSSAT, however, overcomes this limitation by including a weather simulator that can convert monthly statistics into simulated daily weather. In this analysis, the weather is simulated many different times and the outcome averaged over several growing seasons. The result is more of a long-term yield perspective that will not be unduly influenced by any individual stochastic extreme in the simulation.

The soil data used were adapted by Jawoo Koo and John Dimes (2010) from the *Harmonized World Soil Data Base* (HWSD ver. 1.1) by Batjes et al. (2009). They are simplified to 27 types, each with high, medium, or low levels of soil organic carbon; deep, medium, or shallow rooting depth; and major component of sand, loam, or clay. Some grid cells had more than one soil type represented, and when that was the case, the dominant type was used.

DSSAT has parameters to model different varieties of each crop. For our work, we picked what seemed like an appropriate variety and used it in all locations and time periods investigated.

DSSAT requires the user to input the planting date. For rainfed crops, it is assumed that a crop is planted in the first month of a four-month period in which monthly average maximum temperature does not exceed 37°C (about 99°F), the monthly average minimum temperature does not drop below 5°C (about 41°F), and monthly total precipitation is not less than 60 millimeters.

In the tropics, the planting month begins with the rainy season. The particular mechanism for determining the start of the rainy season at any location is to look for the block of four months that gets the most rainfall. The month before that block is called the beginning of the rainy season. For irrigated crops, the first choice is the rainfed planting month.

DSSAT has an option to include CO<sub>2</sub> fertilization effects at different levels of CO<sub>2</sub> atmospheric concentration. For this study, all results use a 369 parts per million setting, which is the concentration in the early 2000s. A short summary of the reasons for and against including CO<sub>2</sub> fertilization is contained in Nelson et al. (2010, 14, text and footnote):

Plants produce more vegetative matter as atmospheric concentrations of CO<sub>2</sub> increase. The effect depends on the nature of the photosynthetic process used by the plant species. So-called C3 plants use CO<sub>2</sub> less efficiently than C4 plants, so C3 plants are more sensitive to higher concentrations of CO<sub>2</sub>. It remains an open question whether these laboratory results translate to actual field conditions. A recent report on field experiments on CO<sub>2</sub> fertilization (Long et al. 2006) finds that the effects in the field are approximately 50 percent less than in experiments in enclosed containers. Another report (Zavala et al. 2008) finds that higher levels of atmospheric CO<sub>2</sub> increase the susceptibility of soybean plants to the Japanese beetle and of maize to the western corn rootworm. Finally, a recent study (Bloom et al. 2010) finds that higher CO<sub>2</sub> concentrations inhibit the assimilation of nitrate into organic nitrogen compounds. So the actual field benefits of CO<sub>2</sub> fertilization remain uncertain.

Some use of nitrogen fertilizer is assumed in all our crop models. For almost all countries in Africa, the level of use is 20 kilograms of nitrogen per hectare (regardless of crop). For Madagascar and parts of South Africa, the level is 100 kilograms of nitrogen per hectare (regardless of crop). Levels were set appropriately for the rest of the world in the global modeling.

DSSAT is used in two ways in this monograph. It is used directly for each country and for the region to compute yields under the climate of 2000 and the climate of 2050. DSSAT is also used to provide results for each country of the world so that IMPACT can control for climate effects. The global work and the regional work were very similar though not perfectly identical because they were produced by two different teams. One example of the differences is the spatial resolution, which was 15 arc-minutes (30 kilometers) for the global team and 5 arc-minutes (10 kilometers) for the regional team. Some of the

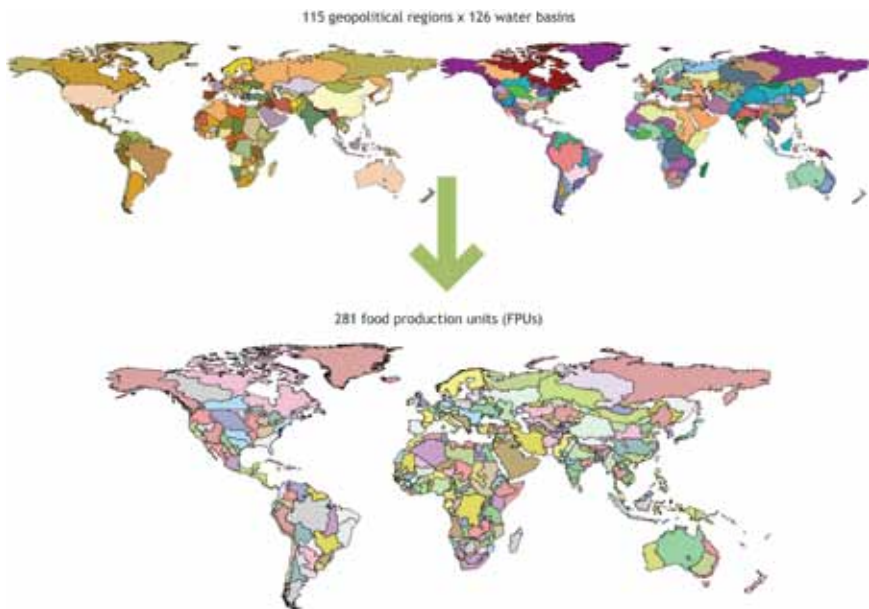
crops for East Africa were modeled by the global team, which is why the resolution in the maps varies between crops in some cases.

## IMPACT

The IMPACT model was initially developed to project global food supply, food demand, and food security to the year 2020 and beyond (Rosegrant et al. 2008). It is a partial equilibrium agricultural model with 32 crop and livestock commodities, including cereals, soybeans, roots and tubers, meats, milk, eggs, oilseeds, oilcakes and meals, sugar, and fruits and vegetables. IMPACT has 115 regions, which are usually countries (though in a few cases several countries are aggregated together, and in rare cases, a country may be subdivided), with specified supply, demand, and prices for agricultural commodities.

Large regions are further divided into major river basins. The result, portrayed in Figure 2.2, is 281 spatial units called food production units (FPUs). The model links the various countries and regions through international trade, using a series of linear and nonlinear equations to approximate the underlying

**FIGURE 2.2** International Model for Policy Analysis of Agricultural Commodities and Trade (IMPACT) unit of analysis, the food production unit (FPU)



production and demand relationships. World agricultural commodity prices are determined annually at levels that clear international markets. Growth in crop production in each country is determined by crop and input prices, exogenous rates of productivity growth and area expansion, investment in irrigation, and water availability. Demand is a function of prices, income, and population growth. We distinguish four categories of commodity demand: food, feed, biofuels feedstock, and other uses.

### **From DSSAT to IMPACT**

For input into the IMPACT model, DSSAT is run for five crops—rice, wheat, maize, soybeans, and groundnuts—at 15-arc-minute intervals for the locations where the SPAM dataset shows that each crop is currently grown. The results from this analysis are then aggregated to the IMPACT FPU level.

In extending these results to other crops in IMPACT, the primary assumption is that plants with the same photosynthetic metabolic pathway will react similarly to any given climate change effect in a particular geographic region. Millet, sorghum, sugarcane, and maize all use the C<sub>4</sub> pathway. Millet and sugarcane are assumed to have the same productivity effects from climate change as maize in the same geographic regions. Sorghum effects for the Africa region were modeled explicitly, but for the rest of the world the maize productivity effects were assumed to apply to sorghum as well. The remainder of the crops use the C<sub>3</sub> pathway. The climate effects for the C<sub>3</sub> crops not directly modeled in DSSAT follow the average from wheat, rice, soy, and groundnuts from the same geographic region, with the following two exceptions. The IMPACT commodities of “other grains” and dryland legumes are directly mapped to the DSSAT results for wheat and groundnuts, respectively.

### **Income and Population Drivers**

Differences in gross domestic product (GDP) and population growth define the overall scenarios, with all other driver values remaining the same across the three scenarios (Table 2.2). The GDP and population growth rates combine to generate the three scenarios of per capita GDP growth. The results by region are shown in Table 2.3. The baseline scenario has just over 9 billion people in 2050; the optimistic scenario results in a substantially smaller number, 7.9 billion; the pessimistic scenario results in 10.4 billion people. For developed countries, the differences among the three scenarios are relatively small, with



**TABLE 2.2** Gross domestic product (GDP) and population choices for the three overall scenarios

Category	Pessimistic	Baseline	Optimistic
GDP (constant 2000 US\$)	Lowest of the four GDP growth rate scenarios from the Millennium Ecosystem Assessment GDP scenarios (Millennium Ecosystem Assessment 2005) and the rate used in the baseline (next column)	Based on rates from a World Bank Economics of Adaptation to Climate Change study (World Bank 2010), updated for Africa south of the Sahara and South Asian countries	Highest of the four GDP growth rates from the Millennium Ecosystem Assessment GDP scenarios (Millennium Ecosystem Assessment 2005) and the rate used in the baseline (previous column)
Population	UN High variant, 2008 revision	UN medium variant, 2008 revision	UN low variant, 2008 revision

Source: Nelson et al. (2010).

**TABLE 2.3** Global average scenario per capita gross domestic product growth rate, 1990–2000 and 2010–2050 (percent per year)

Category	1990–2000	2010–2050		
		Pessimistic	Baseline	Optimistic
Developed countries	2.7	0.74	2.17	2.56
Developing countries	3.9	2.09	3.86	5.00
Low-income developing countries	4.7	2.60	3.60	4.94
Middle-income developing countries	3.8	2.21	4.01	5.11
World	2.9	0.86	2.49	3.22

Sources: *World Development Indicators* for 1990–2000 (World Bank 2009) and Nelson et al. (2010) calculations for 2010–2050.

little overall population growth: population ranges from just over 1 billion to 1.3 billion in 2050, compared to 1 billion in 2010. For the developing countries as a group, the total 2010 population of 5.8 billion becomes 6.9–9 billion in 2050, depending on scenario.

As Table 2.4 shows, average world per capita income, beginning at \$6,600 in 2010, ranges from \$8,800 to \$23,800 in 2050, depending on scenario.<sup>3</sup> The gap between average per capita income in developed and developing countries is large in 2010: developing countries' per capita income is only 5.6 percent of that in developed countries. Regardless of scenario, the relative difference is

3 All references to dollars are to constant 2000 US dollars.

**TABLE 2.4** Summary statistics for population and per capita gross domestic product, 2010 and 2050

Category	2010	2050		
		Optimistic	Baseline	Pessimistic
Population (millions)				
World	6,870	7,913	9,096	10,399
Developed countries	1,022	1,035	1,169	1,315
Developing countries	5,848	6,877	7,927	9,083
Middle-income developing countries	4,869	5,283	6,103	7,009
Low-income developing countries	980	1,594	1,825	2,074
East Africa	361.1	879.4	777.1	681.6
Southern Africa	141.7	276.2	240.2	207.0
West Africa	300.5	697.0	618.5	545.0
Income per capita (2000 US\$)				
World	6,629	23,760	17,723	8,779
Developed countries	33,700	93,975	79,427	43,531
Developing countries	1,897	13,190	8,624	3,747
Middle-income developing countries	2,194	15,821	10,577	4,531
Low-income developing countries	420	4,474	2,094	1,101
East Africa	204	565	1,161	1,778
Southern Africa	1,961	2,725	5,892	11,499
West Africa	363	816	1,695	3,185

Source: Nelson et al. (2010).

Notes: 2010 income per capita is for the baseline scenario. US\$ = US dollars.

reduced over time: the developing-country income increases to between 8.6 percent and 14.0 percent of developed-country income in 2050, depending on the overall scenario. Middle- and low-income developing countries' 2010 per capita income values are 6.5 percent and 2.6 percent, respectively, of the developed-country income. By 2050, the share increases to between 10.4 percent and 16.8 percent for middle-income developing countries, depending on the overall scenario. For the low-income developing countries, however, the 2050 ratios remain low—between 2.5 percent and 4.8 percent.

The reader should be somewhat cautious in interpreting the results based on the three different scenarios. The optimistic scenario is optimistic not just

for one country but for the entire world. This means that we cannot look at the impact from assuming that a single country is able to reduce its population growth rate or increase its GDP while the rest of the world continues at the same GDP and population growth rate. Rather, we have only the case in which all countries have a higher GDP and lower population growth rate. This means that changing scenarios changes supply and demand for the whole world, not just for one country.

### **Metrics for Human Well-being**

Physical human well-being has many determinants. Calorie availability is a key element in low-income countries, where malnutrition and poverty are serious problems. Distribution, access, and supporting resources can enhance or reduce an individual's calorie availability. Similarly, child malnutrition has many determinants, including calorie intake (Rosegrant et al. 2008). The relationship used to estimate the number of malnourished children is based on a cross-country regression relationship estimated by Smith and Haddad (2000) that takes into account female access to secondary education, the quality of maternal and child care, and health and sanitation.<sup>4</sup> The IMPACT model provides data on per capita calorie availability by country; the other determinants are assumed to remain the same across the overall scenarios.

A number of countries included in this monograph show rising GDP per capita yet falling mean calorie consumption. This can be partially explained by noting that staple foodcrops increase in price. For example, maize prices are projected to nearly double from 2010 to 2050, rice prices are projected to be 80 percent higher, and wheat prices are expected to be more than 50 percent higher. People living on already-low GDP per capita spend a very large portion of their income on food, so income gains would be offset in part by price increases. However, the drop in consumption observed in the IMPACT model results also reflects the sensitivity to the model in response to elasticities that

---

4 Because it is a partial equilibrium model, IMPACT has no feedback mechanisms from climate change effects on productivity to income. This means that it cannot estimate directly the poverty effects of agricultural productivity declines from climate change. However, the reduced form function that relates child malnutrition to calorie availability and other determinants implicitly includes the effects of real income change on child malnutrition. Hertel, Burke, and Lobell (2010) use a general equilibrium model to estimate explicitly the effects of climate change on poverty. They find that the poverty impacts to 2030 “depend as much on where impoverished households earn their income as on the agricultural impacts themselves, with poverty rates in some non-agricultural household groups rising by 20–50 percent in parts of Africa and Asia under these price changes, and falling by equal amounts for agriculture-specialized households elsewhere in Asia and Latin America.”

**TABLE 2.5** Noncaloric determinants of global child malnutrition, 2010 and 2050

Country category	Clean water access (percent) <sup>a</sup>		Female schooling (percent) <sup>b</sup>		Female relative life expectancy <sup>c</sup>	
	2010	2050	2010	2050	2010	2050
Middle-income countries	86.8	98.4	71.6	81.7	1.066	1.060
Low-income countries	69.0	85.8	54.9	61.6	1.044	1.048

Sources: Population-weighted aggregations in Nelson et al. (2010) based on data from 2000 with expert extrapolations to 2050. Original data sources include the World Health Organization's Global Database on Child Growth and Malnutrition; the United Nations Administrative Committee on Coordination–Subcommittee on Nutrition; the World Bank's *World Development Indicators* (World Bank 2009); FAOSTAT (FAO 2010); and the United Nations Educational, Scientific, and Cultural Organization's UNESCOSTAT database. Aggregations are weighted by population shares and are based on the baseline population growth scenario.

<sup>a</sup>Share of population with access to safe water.

<sup>b</sup>Total female enrollment in secondary education (any age group) as a percentage of the female age group corresponding to national regulations for secondary education.

<sup>c</sup>Ratio of female to male life expectancy at birth.

were estimated with uncertainty, as well as the reality that elasticities do not necessarily function well for nonmarginal changes.

Table 2.5 shows the 2010 and 2050 values for the noncaloric determinants of child malnutrition aggregated to low- and middle-income countries. The small decline in female relative life expectancy in 2050 for the middle-income countries will be caused primarily by a decline in China, where it is expected that male life expectancy will gradually move up rather than female life expectancy moving down.

### **Agricultural Vulnerability to Climate Change**

There are many dimensions to agricultural vulnerability to climate change: vulnerability of agricultural systems, communities, households, and individuals to climate change. Vulnerability is influenced by the degree of exposure and sensitivity to that exposure. Household-level vulnerability is most often associated with threats to livelihoods. Livelihoods can be inadequate because of resource constraints and low productivity (e.g., farmers with too little land and no access to fertilizer) or because they operate in a risky environment (e.g., droughts that cause harvest failure).

Potential impacts of climate change on vulnerability to food insecurity include both direct nutritional effects (changes in consumption quantities and composition) and livelihood effects (changes in employment opportunities and the cost of acquiring adequate nutrition). Climate change can affect each of these dimensions. This monograph focuses on the productivity effects of climate change that translate into changes in calorie availability and to the

**TABLE 2.6** Mean price elasticities used for east and central African countries in IMPACT, 2010 and 2050

Food	2010		2050	
	Income	Own price	Income	Own price
Beef	0.945	-0.823	0.778	0.720
Lamb	0.536	-0.481	0.417	-0.425
Maize	0.200	-0.710	0.153	-0.689
Cassava	0.091	-0.679	-0.005	-0.632
Sorghum	0.267	-0.487	0.091	-0.401
Wheat	0.585	-0.893	0.485	-0.842

Source: Authors' calculations.

Notes: Averages are weighted averages based on national consumption of each food item in 2000. IMPACT = International Model for Policy Analysis of Agricultural Commodities and Trade.

effects on child malnutrition. At this point the methodology and data to provide quantitative estimates of livelihood vulnerability are not available.

For the calorie estimates used in this monograph, price and income elasticities from an earlier global study were used (Nelson et al. 2010). Table 2.6 presents a weighted average of these elasticities for important crops in the east and central African countries included in this monograph. The own-price elasticities are large (in absolute terms) relative to other studies. Other studies of the own-price elasticities for starchy staples report values that range from  $-0.05$  to  $-0.3$ , whereas the elasticities in Table 2.6 are in the range of  $-0.40$  to  $-0.89$ . The global modeling results in large price increases, which offset the effects of income increases in the pessimistic scenario and in some cases in the optimistic scenario as well.

Although it was not possible to recalibrate elasticities and generate all-new results for this monograph in a timely manner, the IMPACT model is being revised continuously, and future results will be based on improved elasticities.

### Travel Time Maps

We developed databases that show simulated travel time to towns and cities of various sizes. The analysis begins with information on how long it would take someone to travel through a small region, roughly 10 kilometers on a side. This information is developed by overlaying various geographic information system (GIS) datasets, including ones for roads, rivers and other water bodies, urban areas, and international boundaries. Each feature has a particular speed associated with it, and there is a default speed for areas without detailed information.

Once the time to travel across the regions is developed, the only other data required is the location of the towns and cities of interest. We used cities and towns from two sources: CIESIN (2004) and the *World Gazetteer* (Helders 2005). ArcView 3.2 was used to calculate the shortest travel time to any point in the specified cities and towns dataset.

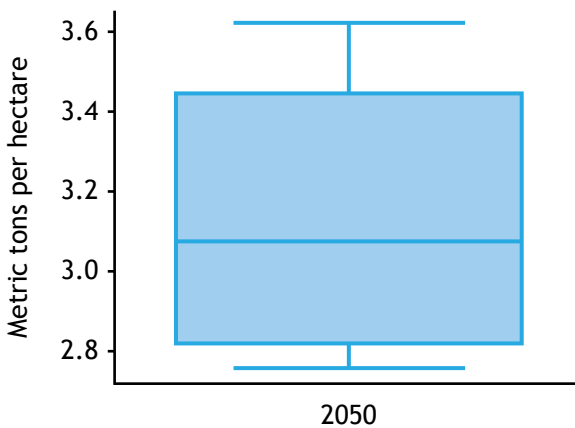
### Box-and-Whisker Graphs

A box-and-whisker graph summarizes a variety of information for a variable in a relatively straightforward diagram. A sample box-and-whisker graph is shown in Figure 2.3. The horizontal lines at the top and bottom of the diagram are the “whiskers” and show the minimum and maximum values of the variable. The top and bottom edges of the rectangle, the “box,” show the 75th and 25th percentiles, respectively, of the variable under consideration. The horizontal divider line inside the box is the median value of the data.

These graphs were generated using Stata (StataCorp 2009) with Tukey’s (1977) formula for setting the upper and lower whisker values, which Stata calls “adjacent values.”

Now that we have given a general overview of the models and some of the data reviewed in this monograph, we are ready to see the results of the models applied to each of the countries studied in the chapters that follow.

**FIGURE 2.3** Sample box-and-whisker graph



Sources: Authors, using StataCorp (2009) and Tukey (1977).

## References

- Batjes, N., K. Dijkshoorn, V. van Engelen, G. Fischer, A. Jones, L. Montanarella, M. Petri, S. Prieler, E. Teixeira, and X. Shi. 2009. Harmonized World Soil Database. Laxenburg, Austria: International Institute for Applied Systems Analysis (IIASA).
- Bloom, A. J., M. Burger, R. Assensio, J. Salvador, and A. B. Cousins. 2010. "Carbon Dioxide Enrichment Inhibits Nitrate Assimilation in Wheat and Arabidopsis." *Science* 328: 899–902.
- CIESIN (Center for International Earth Science Information Network, Columbia University), Columbia University, IFPRI (International Food Policy Research Institute), World Bank, and CIAT (Centro Internacional de Agricultura Tropical). 2004. *Global Rural–Urban Mapping Project, Version 1 (GRUMPv1)*. Palisades, NY, US: Socioeconomic Data and Applications Center (SEDAC), Columbia University. <http://sedac.ciesin.columbia.edu/gpw>.
- Helders, S. 2005. *World Gazetteer Database*. Accessed June 7, 2007. <http://world-gazetteer.com/>.
- Hertel, T. M., M. B. Burke, and D. B. Lobell. 2010. "The Poverty Implications of Climate-Induced Crop Yield Changes by 2030." *Global Environmental Change* 20 (4): 577–585.
- Jones, J. W., G. Hoogenboom, C. H. Porter, K. J. Boote, W. D. Batchelor, L. A. Hunt, P. W. Wilkens, U. Singh, A. J. Gijsman, and J. T. Ritchie. 2003. "The DSSAT Cropping System Model." *European Journal of Agronomy* 18 (3–4): 235–265.
- Jones, P. G., P. K. Thornton, and J. Heinke. 2009. "Generating Characteristic Daily Weather Data Using Downscaled Climate Model Data from the IPCC's Fourth Assessment." Project report for the International Livestock Research Institute (ILRI). Available at [http://www.ccafs-climate.org/pattern\\_scaling](http://www.ccafs-climate.org/pattern_scaling).
- Koo, J., and J. Dimes. 2010. HC27 Generic Soil Profile Database. Version 1, July. International Food Policy Research Institute, Washington, DC. <http://hdl.handle.net/1902.1/20299>.
- Long, S. P., E. A. Ainsworth, A. D. B. Leakey, J. Nosberger, and D. R. Ort. 2006. "Food for Thought: Lower-than-Expected Crop Yield Stimulation with Rising CO<sub>2</sub> Concentrations." *Science* 312 (5782): 1918–1921. doi:10.1126/science.1114722. <http://www.sciencemag.org/cgi/content/abstract/312/5782/1918>.
- Millennium Ecosystem Assessment. 2005. *Ecosystems and Human Well-being: Synthesis*. Washington, DC: Island Press. <http://www.maweb.org/en/Global.aspx>.
- Nakicenovic, N., et al. 2000. *Special Report on Emissions Scenarios: A Special Report of Working Group III of the Intergovernmental Panel on Climate Change*. Cambridge: Cambridge University Press. <http://www.grida.no/climate/ipcc/emission/index.htm>.
- Nelson, G. C., M. W. Rosegrant, A. Palazzo, I. Gray, C. Ingersoll, R. Robertson, S. Tokgoz, et al. 2010. *Food Security, Farming, and Climate Change to 2050: Scenarios, Results, Policy Options*. Washington, DC: International Food Policy Research Institute.

- Rosegrant, M. W., S. Msangi, C. Ringler, T. B. Sulser, T. Zhu, and S. A. Cline. 2008. *International Model for Policy Analysis of Agricultural Commodities and Trade (IMPACT): Model Description*. Washington, DC: International Food Policy Research Institute. <http://www.ifpri.org/themes/impact/impactwater.pdf>.
- Smith, L., and L. Haddad. 2000. *Explaining Child Malnutrition in Developing Countries: A Cross-Country Analysis*. Washington, DC: International Food Policy Research Institute.
- StataCorp. 2009. Stata: Release 11. Statistical Software. College Station, TX, US.
- Tukey, J. W. 1977. *Exploratory Data Analysis*. Reading, MA, US: Addison–Wesley.
- UNPOP (United Nations Department of Economic and Social Affairs–Population Division). 2009. *World Population Prospects: The 2008 Revision*. New York. <http://esa.un.org/unpd/wpp>.
- World Bank. 2009. *World Development Indicators*. Accessed May 2011. <http://data.worldbank.org/data-catalog/world-development-indicators>.
- . 2010. *Economics of Adaptation to Climate Change: Synthesis Report*. Washington, DC. <http://climatechange.worldbank.org/content/economics-adaptation-climate-change-study-homepage>.
- You, L., and S. Wood. 2006. “An Entropy Approach to Spatial Disaggregation of Agricultural Production” *Agricultural Systems* 90 (1–3): 329–347.
- You, L., S. Wood, and U. Wood-Sichra. 2006. “Generating Global Crop Distribution Maps: From Census to Grid.” Paper presented at the International Association of Agricultural Economists Conference, Brisbane, Australia, August 11–18.
- . 2009. “Generating Plausible Crop Distribution and Performance Maps for Sub-Saharan Africa Using a Spatially Disaggregated Data Fusion and Optimization Approach.” *Agricultural Systems* 99 (2–3): 126–140.
- Zavala, J. A., C. L. Casteel, E. H. DeLucia, and M. R. Berenbaum. 2008. “Anthropogenic Increase in Carbon Dioxide Compromises Plant Defense against Invasive Insects.” *Proceedings of the National Academy of Sciences* 105 (13): 5129–5133. doi:10.1073/pnas.0800568105. <http://www.pnas.org/content/105/13/5129.abstract>.